



NRC Publications Archive Archives des publications du CNRC

Flexural toughness as an attribute for impact damage evaluation of composite laminates

Alemi-Ardakani, Mohammad; Milani, Abbas S.; Yannacopoulos, Spiro;
Trudel-Boucher, David; Shokouhi, Golnaz

This publication could be one of several versions: author's original, accepted manuscript or the publisher's version. /
La version de cette publication peut être l'une des suivantes : la version prépublication de l'auteur, la version
acceptée du manuscrit ou la version de l'éditeur.

Publisher's version / Version de l'éditeur:

*Proceedings of the ASME 2011 International Mechanical Engineering Congress &
Exposition: IMECE2011, 2011-11-11*

NRC Publications Record / Notice d'Archives des publications de CNRC:

<https://nrc-publications.canada.ca/eng/view/object/?id=1029e71b-94e1-4bc1-9afb-499396bf495f>
<https://publications-cnrc.canada.ca/fra/voir/objet/?id=1029e71b-94e1-4bc1-9afb-499396bf495f>

Access and use of this website and the material on it are subject to the Terms and Conditions set forth at

<https://nrc-publications.canada.ca/eng/copyright>

READ THESE TERMS AND CONDITIONS CAREFULLY BEFORE USING THIS WEBSITE.

L'accès à ce site Web et l'utilisation de son contenu sont assujettis aux conditions présentées dans le site

<https://publications-cnrc.canada.ca/fra/droits>

LISEZ CES CONDITIONS ATTENTIVEMENT AVANT D'UTILISER CE SITE WEB.

Questions? Contact the NRC Publications Archive team at

PublicationsArchive-ArchivesPublications@nrc-cnrc.gc.ca. If you wish to email the authors directly, please see the first page of the publication for their contact information.

Vous avez des questions? Nous pouvons vous aider. Pour communiquer directement avec un auteur, consultez la première page de la revue dans laquelle son article a été publié afin de trouver ses coordonnées. Si vous n'arrivez pas à les repérer, communiquez avec nous à PublicationsArchive-ArchivesPublications@nrc-cnrc.gc.ca.



ABSTRACT

Popularity and application of composite materials are increasing in several industries including transportation, construction and aerospace. The mechanical properties of these materials should be known to engineers to be able to design/select new products reliably. Impact resistance is one of the mechanical properties which have been studied extensively over the past years and still is an ongoing topic in the composite research. Since analytical solutions have not been fully developed for the impact characterization of anisotropic materials, researchers often perform mechanical testing in conjunction with visual inspection methods to investigate the impact behavior of composite materials. The present study shows that a differential flexural toughness can be considered as a reliable measure at the design/material selection level for the damage evaluation of composite laminates. For this purpose, a series of drop-weight impact tests with 200J energy were performed on specimens made of four different stacking configurations of TWINTEx® and unidirectional laminates (polypropylene and glass fiber commingled composites). These tests were done according to ASTM D7136. The damaged areas of impacted specimens were measured with an image analysis method. Following, four-point flexural tests were carried out based on ASTM D7264 on both non-impacted and impacted specimens. Finally, damaged area and flexural toughness, along with a set of other commonly used mechanical properties, were selected as different attributes for damage evaluation. Comparison of results under different criteria showed that in the present case study, visual inspection may not be a good way to predict the post-impact properties of the tested specimens and can be a misleading method. On the other hand, a differential flexural toughness measure gives a much clear perspective on the post-impact resistance of the specimens.

INTRODUCTION

In the last two decades, numerous experimental and analytical investigations have been conducted to characterize the mechanical properties of fibre reinforced polymers (FRPs). Impact behavior, especially for the design of high-risk components, has been a main focus of these investigations. The simplest way to investigate damage intensity in an impacted composite is visual investigation [1-6]. Junior et al. [4] developed a perdition model for residual impact strength and tensile modulus properties as a function of observed delamination area due to ballistic impact. The delaminated areas were measured by a digital image analysis of the scanned photos from damage surfaces. KS400 software detected bounds of delaminated regions

automatically based on contrast between delaminated (light grey) and unaffected (dark grey) zones [4]. Similarly, Nunes et al. [5] used Marr–Hildreth segmentation, a low-pass filtration method, for measuring the scanned delaminated damage areas [5]. In this method, A-scan [7] and C-scan [8-14,24] ultrasonic evaluations were used to investigate damaged zones. A relation was established between impact energy and delamination area obtained by means of a pulse-echo immersion method [8].

Aymerich et al. [9] determined the delamination induced in carbon-PEEK laminates due to low-velocity impact using conventional time-of-flight and amplitude C-scans. Matrix cracks were detected with backscattering C-scanning, a method in which the transducer is set at an angle to the laminate plane. Xiong et al. [12] developed a numerical model for post impact compression properties of composite laminates and verified their model by results of an ultrasonic time-of-flight C-scan technique. X-ray images have also been used to investigate damage properties of materials [15-17]. Luo et al. [16] validated their numerical model, which predicted impact damage initiation and propagation in composite plates, with the X-ray images of tested specimens. A newly developed nanocomposite layer was used by Capezzuto et al. [18] to reveal the barely visible impact damages (BVIDs). The semiconductor CuS nano-particles embedded into a polymer matrix showed specific light emission in visible range of the electromagnetic spectrum under UV-light excitation at different wavelengths, which was in turn employed to visualize BVIDs. Infrared thermography has been used to study the impact induced damages recently [19-21]. In this method, the impact event of fiberglass specimens was recorded by a high frame rate infrared thermal camera. Thermoelastic Stress Analysis and Pulse Heating Thermography were then used for post-impact analysis and detection of damage, including fiber fractures and delamination [21]. Gros [22] employed the Eddy-Current approach for the detection of impact damage of CFRP materials. Acoustography is another method used for damage detection [23-25]. Scanning Acoustic Microscopy (SAM) has been also used to monitor the delamination growth under impact loading at different temperatures [25]. Other non-destructive damage detection approaches reported in the literature include Electrical Resistance [26], Electronic Speckle Pattern Interferometry (ESPI) [27], Holographic Interferometry [28], Double Pass Retrodeflection (D Sight) [29] and Optical Deformation and Strain Measurement System (ODSMS) [30].

It is worth mentioning that there is a common problem in most visual inspection methods reviewed above: how to distinguish between different types of failure modes such as matrix cracking, fiber breakage, fiber pull out, fiber-matrix debonding and delamination, and also how to predict the contribution of each mode on the material resistance loss? This study proposes a differential flexural toughness measure as a global attribute to investigate the damage residual properties of impacted laminates. The method still does not distinguish among failure modes, however it provides an aggregative measure to estimate the post-impact resistance of laminates that is often of concern for designers, specially during material selection processes.

EXPERIMENTAL

1. Materials

This case study included four different types of balanced composite laminates. The constituent

material system for each unconsolidated laminate was E-glass fibers and polypropylene (PP) matrix. All the test samples were consolidated using vacuum bagging and had an identical size of 6 mm \times 100 mm \times 150 mm. The only difference between the four laminates was their weave pattern. One laminate was made of unidirectional laminas with glass content of 70 wt% and the other three were made of different woven fabrics with glass content of 60 wt%: plain weave (11/11), twill weave (22/22) and an unbalanced weave (22/11). For brevity, let us assume the codes '1', '2', 'W' and 'UD' correspond to the plain weave, twill weave, unbalanced weave, and unidirectional lamina, respectively. Table (1) shows specifications of the four laminates based on the above coding. In order to have a balanced laminate, unbalanced and UD layers were laid up in a cross-ply configuration ($UD^{0/90}$ and $W^{0/90}$).

Table. 1: Specification of the tested Twintex and UD laminates.

Laminate/Mat. No.	Material of each layer	Lamina Code	Configuration of Sample	Dimensions of Sample (mm)
1	Twintex plain weave (11/11)	1	$[(1)_6]_s$	6 \times 100 \times 150
2	Twintex twill weave (22/22)	2	$[(2)_3]_s$	6 \times 100 \times 150
3	Twintex unbalanced weave (22/11)	W	$[(W^{0/90})_2]_s$	6 \times 100 \times 150
4	Unidirectional	UD	$[(UD^{0/90})_3]_s$	6 \times 100 \times 150

2. Drop-Weight Impact Testing

Drop-weight impact tests were performed on the samples in Table (1) according to the ASTM D7136 standard. The projectile was a 1-inch-hemispherical impactor with 12.35 kg weight. Boundaries of the specimens were clamped with a rectangular rig. The projectile impacted the center of specimens with a velocity of 5.69 m/s and 200J energy. In order to measure the areas of damaged zones as an indicator of damage intensity and its effect on the residual mechanical properties, images were taken from the rear face of specimens. The captured photos were analyzed with an image processing software and a ruler was used to calibrate the length scale in the photos to the actual length unit. For example, for laminate 1, as shown in Figure (1), the measured area by image processing (0.89 in²) was divided by the square of scale factor (0.64) to find the corresponding area in cm². Each damage area was encapsulated by a polygon around the boundary of visible damage zone in the photos. The selection of the corner points of polygon was, however, very sensitive to errors from the operator. In order to reduce the latter effect,

the entire visual measurement process was repeated three times. M1, M2 and M3 in Table (2) refer to the corresponding values for these repeats.

3. Four-Point Flexural Testing

A series of four-point flexural tests (Figure (2)) were performed on impacted and non-impacted samples. The results were subsequently compared to each other to investigate the effect of low-velocity impact on the residual mechanical properties of the laminates. Namely, the Young's modulus, maximum flexural strength and flexural toughness of laminates were measured for both impacted and non-impacted specimens. To increase the reliability of analysis, each test was repeated twice, where according to ASTM D7264 the following configuration was used:

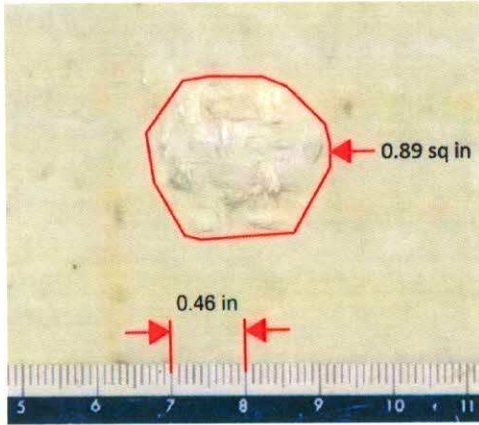


Fig. 1: Measurement system of damaged area (the blue scale is in cm).

- Support span (L) = 100mm,
- Loading span ($L/2$) = 50mm,
- Support span-to-thickness ratio $= \frac{100}{6} \approx \frac{16}{1}$.
- The loading noses and supports have cylindrical contact surfaces of radius 0.5 in.

Force-deflection values were recorded and used to calculate the flexural stress, strain and chord modulus using the following relations [ASTM D7264]:

$$\sigma_f = \frac{3PL}{4bh^2} \quad (1)$$

$$\varepsilon_f = \frac{4.36\delta h}{L^2} \quad (2)$$

$$E_f = \frac{\Delta\sigma_f}{\Delta\varepsilon_f} \quad (3)$$

where,

σ_f : Stress at the outer surface in the load span region, MPa;



Fig. 2: A Twintex laminate under four-point bending.

ε_f : Maximum strain at the outer surface, mm/mm;

E_f : Flexural chord modulus, MPa;

P : Applied force, N;

L : Support span, mm;

b : Width of beam, mm;

h : Thickness of beam, mm; and

δ : Mid-span deflection, mm.

To calculate the flexural modulus of the laminates, a strain range of 0.002 with the start point of 0.001 and the end point of 0.003 has been recommended according to ASTM D7264. In this case, as it can be seen in Figure (3), the linear elastic strain range was selected between 0.5 to 1.5%.

To measure the flexural toughness of the laminates, the area under the stress-extension curves was calculated. In order to compare the flexural toughness of each material up to the same reference point before and after impact, a datum line was plotted from the pick stress of the non-impacted sample data, indicating its ultimate strength point. Then, the area under each curve for both impacted and non-impacted materials were measured up to this line (Figure (4)).

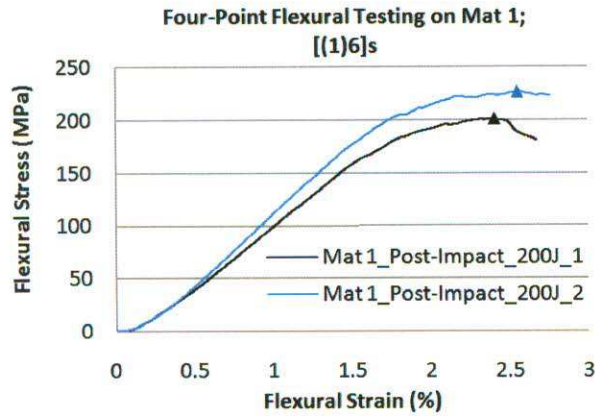


Fig. 3: Flexural stress-strain behavior of Material 1 after 200J impact.

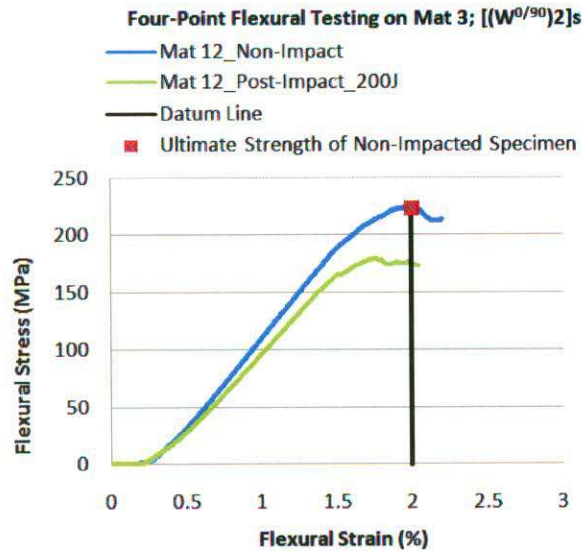
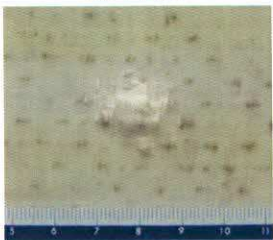
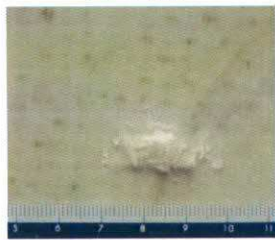






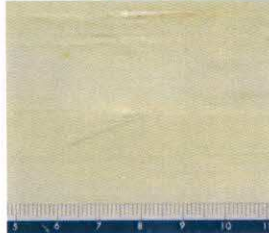
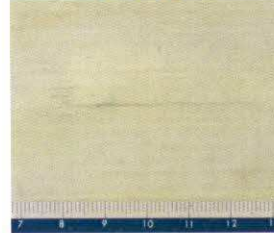
Fig. 4: Datum line from the ultimate strength of non-impacted specimen (Material 3).

Table (2) summarizes graphical results of impact tests on the laminated under study. Figures (5)-(8) also show the obtained mechanical properties. In practice, a designer may encounter a question as to which of these properties to use in order to draw conclusions among different materials (e.g., for selecting the best configuration). For example, Figure (5) suggests that laminate 1 (plain weave) is the best option as it appears to be the strongest before and after impact. It also indicates that the difference between laminates 1 and 2 after impact becomes narrower. In other words, the ultimate strength of laminate 2 is not as sensitive to impact as the other laminates are. On the other hand, Figure (6) shows that the chord modulus of laminate 4 (UD) is the highest before impact, but it drops significantly after impact. Thus, laminate 4 may be considered as a suitable material option for a disposable/low risk component with a low post-impact stiffness requirement. However, it cannot be recommended for a sensitive/high risk component. Figure (7) clearly shows laminate 1 is the toughest material. The interesting point from this figure is that the difference between the toughness of all laminates remains virtually constant before and after the same impact, which means this mechanical property may be a very clear measure to distinguish among different laminate configurations with regards to their both pre- and post impact resistance. Figure (8) demonstrates the rear face visual damage investigation results which seem to present inconsistencies: laminate 4 from the four-point bending test has the lowest toughness, yet no severe rear face damage has been observed. This suggests that the impact energy in this laminate has been dissipated through internal damage mechanisms (matrix cracking, delamination, fiber breakage and pull-out). However, none of these damage modes are visible on the outer surfaces and hence, it is not correct to correlate the rear face damaged area to residual mechanical properties directly.

RESULTS AND DISCUSSION

Table. 2: Results of impact testing on the selected laminates.

Mat. #	Configuration	Impact Energy	Back Face Damaged Zone		Damaged Area (cm ²)	Average of Damaged Area (cm ²)
			Repeat #1	Repeat #2		
1	[(1)6] _s	200J	63-1-200	64-1-200	Area #63: M ₁ =3.33 M ₂ =3.24 M ₃ =3.75	3.50
					Area #64: M ₁ = 3.24 M ₂ = 3.51 M ₃ =3.93	

2	[(2) ₃] _s	200J	85-2-200	86-2-200	Area #85: M ₁ =3.79 M ₂ =3.79 M ₃ =3.65	3.03
					Area #86: M ₁ = 2.36 M ₂ = 2.36 M ₃ =2.22	
3	[(W ^{0/90}) ₂] _s	200J	95-3-200	96-3-200	Area #95: M ₁ =3.14 M ₂ =2.77 M ₃ =3.05	3.07
					Area #96: M ₁ = 2.91 M ₂ = 3.28 M ₃ =3.24	
4	[(UD ^{0/90}) ₃] _s	200J	79-4-200	80-5-200	Area #79: M ₁ =0.23 M ₂ =0.23 M ₃ =0.55	0.44
					Area #80: M ₁ = 0.83 M ₂ = 0.14 M ₃ =0.65	

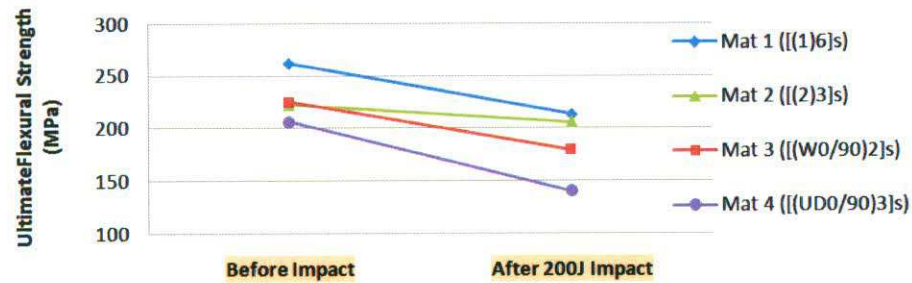


Fig. 5: Ultimate flexural strength of tested laminates before and after impact loading.

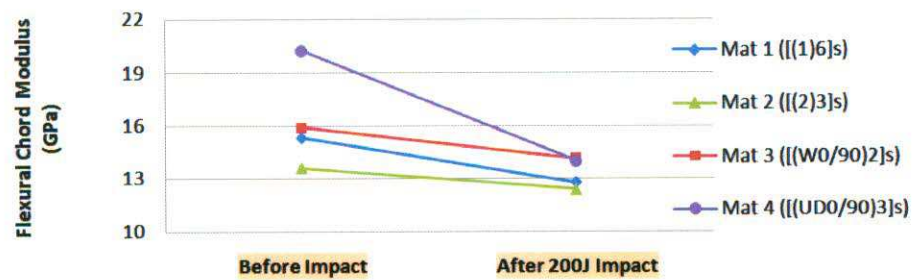


Fig. 6: Young modulus of tested laminates before and after impact loading.

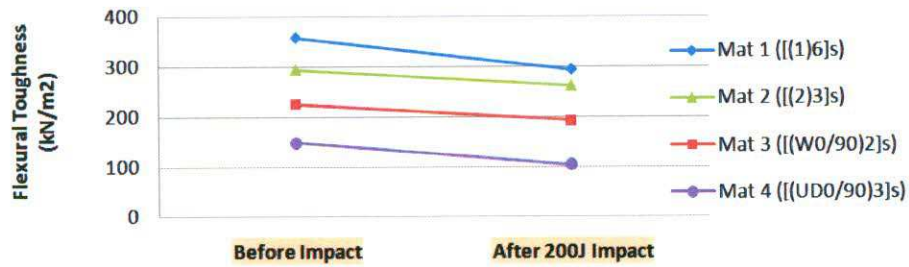


Fig. 7: Flexural toughness of tested laminates before and after impact loading.

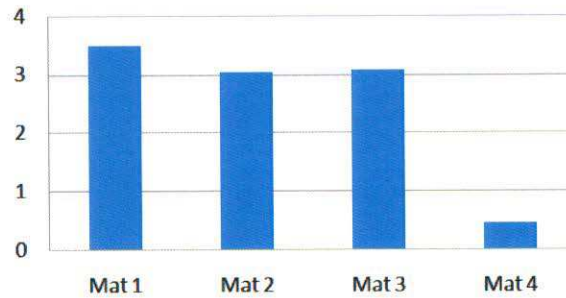


Fig. 8: Comparison of visible damaged areas (cm²) for Materials 1-4.

CONCLUSION

Impact resistance of light-weight composites can be one of the main criteria for designers in choosing their optimum configurations. Accordingly, a representative design attribute for damage evaluation of laminates should be used to clearly compare their pre- and post- impact mechanical performance. This study suggested such an attribute for comparing a set of PP/E-glass laminates with different fiber architectures. A series of impact and flexural testing were performed on the selected laminates. Four criteria were taken into account; a) ultimate flexural strength, b) flexural chord modulus, c) flexural toughness and d) visible rear face damage area. Among these, flexural toughness appeared to be a clear measure as the corresponding comparisons did not vary before and after impact for all samples (i.e., it was independent of the impact energy in this case study). The other important point about this measure was that it comprises both the deflection history and strength of the material. The difference in flexural toughness value before and after an impact event can indicate an approximation of the amount of work needed by the impactor to impose permanent deformation/damage into the specimen (or conversely

speaking, it can be used to predict the capacity of the material to absorb impact energy).

For more complex cases, future research includes the introduction of a multi-objective material selection framework for impact applications, where more than one criterion may be included in the selection process.

ACKNOWLEDGEMENTS

The authors would like to acknowledge the staff from AS Composite and IMI-NRC for providing the test samples and directing the experimental part of the work. Financial support from the Natural Sciences and Engineering Research Council (NSERC) of Canada is greatly acknowledged.

REFERENCES

- [1] M. Alemi Ardakani, A. Afaghi Khatibi, H. Parsaiyan, "An Experimental Study on the Impact Resistance of Glass-Fiber-Reinforced Aluminum (Glare) Laminates", 17th International Conference on Composite Materials, Edinburgh, UK, July 27-31, (2009).
- [2] Tien-Wei Shyr, Yu-Hao Pan, "Impact resistance and damage characteristics of composite laminates", Composite Structures, 62 (2003) 193-203.

- [3] Caneva, S. Olivieri, C. Santulli & G. Bonifazi, "Impact damage evaluation on advanced stitched composites by means of acoustic emission and image analysis", *Composite Structures*, 25 (1993) 121-128.
- [4] J.E.L. da Silva Junior, S. Paciornik, J.R.M. d'Almeida, "Evaluation of the effect of the ballistic damaged area on the residual impact strength and tensile stiffness of glass-fabric composite materials", *Composite Structures*, 64 (2004) 123-127.
- [5] L.M. Nunes, S. Paciornik, J.R.M. d'Almeida, "Evaluation of the damaged area of glass-fiber-reinforced epoxy-matrix composite materials submitted to ballistic impacts", *Composites Science and Technology*, 64 (2004) 945-954.
- [6] K. Azouaoui, Z. Azari, G. Pluvinaige, "Evaluation of impact fatigue damage in glass-epoxy composite laminate", *International Journal of Fatigue*, 32 (2010) 443-452.
- [7] Ramin Hosseinzadeh, Mahmood Mehrdad Shokrieh, Larry Lessard, "Damage behavior of fiber reinforced composite plates subjected to drop weight impacts", *Composites Science and Technology*, 66 (2006) 61-68.
- [8] M.V. Hosur, C.R.L. Murthy, T.S. Ramamurthy, Anita Shet, "Estimation of impact-induced damage in CFRP laminates through ultrasonic imaging", *NDT&E International*, 31 (1998) 359-374.
- [9] F. Aymerich, S. Meili, "Ultrasonic evaluation of matrix damage in impacted composite laminates", *Composites: Part B*, 31 (2000) 1-6.
- [10] H. Kaczmarek, S. Maison, "Comparative ultrasonic analysis of damage in CFRP under static indentation and low-velocity impact", *Composites Science and Technology*, 51 (1994) 11-26.
- [11] W. Riedel, H. Nahme, D.M. White, R.A. Clegg, "Hypervelocity impact damage prediction in composites: Part II—experimental investigations and simulations", *International Journal of Impact Engineering*, 33 (2006) 670-680.
- [12] Y. Xiong, C. Poon, P. V. Straznicky, H. Vietinghoff, "A prediction method for the compressive strength of impact damaged composite laminates", *Composite Structures*, 30 (1995) 357-367.
- [13] T. Gomez-del Rio, R. Zaera, E. Barbero, C. Navarro, "Damage in CFRPs due to low velocity impact at low temperature", *Composites: Part B*, 36 (2005) 41-50.
- [14] A.N. Palazotto, L.N.B. Gummadi, U.K. Vaidya, E.J. Herup, "Low velocity impact damage characteristics of Z-fiber reinforced sandwich panels - an experimental study", *Composite Structures*, 43 (1999) 275-288.
- [15] W.A. de Moraes, S.N. Monteiro, J.R.M. d'Almeida, "Evaluation of repeated low energy impact damage in carbon-epoxy composite materials", *Composite Structures*, 67 (2005) 307-315.
- [16] R.K. Luo, E.R. Greem, C.J. Morrison, "An approach to evaluate the impact damage initiation and propagation in composite plates", *Composite: Part B*, 32 (2001) 513-520.
- [17] R.K. Luo, "The evaluation of impact damage in a composite plate with a hole", *Composites Science and Technology*, 60 (2000) 49-58.
- [18] F. Capezzuto, F. Ciampa, G. Carotenuto, M. Meo, Eva Milella, F. Nicolais, "A smart multifunctional polymer nanocomposites layer for the estimation of low-velocity impact damage in composite structures", *Composite Structures*, 92 (2010) 1913-1919.
- [19] Carosena Meola, Giovanni M. Carlomagno, "Impact damage in GFRP: New insights with infrared thermography", *Composites: Part A*, 41 (2010) 1839-1847.
- [20] Igor M. De Rosa, Carlo Santulli, Fabrizio Sarasini, Marco Valente, "Post-impact damage characterization of hybrid configurations of jute/glass polyester laminates using acoustic emission and IR thermography", *Composites Science and Technology*, 69 (2009) 1142-1150.
- [21] Lovre Krstulovic-Opara, Branko Klarin, Pedro Neves, Zeljko Domazet, "Thermal imaging and Thermoelastic Stress Analysis of impact damage of composite materials", *Engineering Failure Analysis*, 18 (2011) 713-719.
- [22] Xavier E. Gros, "An eddy current approach to the detection of damage caused by low-energy impacts on carbon fibre reinforced materials", *Materials & Design*, 16 (1995) 167-173.
- [23] R. Butler, D.P. Almond, G.W. Hunt, B. Hu, N. Gathercole, "Compressive fatigue limit of impact damaged composite laminates", *Composites: Part A*, 38 (2007) 1211-1215.
- [24] Shang-Lin Gao, Jang-Kyo Kim, "Scanning acoustic microscopy as a tool for quantitative characterisation of damage in CFRPs", *Composites Science and Technology*, 59 (1999) 345-354.
- [25] K.H. Im, C.S. Cha, S.K. Kim, I.Y. Yang, "Effects of temperature on impact damages in CFRP composite laminates", *Composites: Part B*, 32 (2001) 669-682.
- [26] Shoukai Wang, D.D.L. Chung, Jaycee H. Chung, "Impact damage of carbon fiber polymer-matrix composites, studied by

- electrical resistance measurement”, *Composites: Part A*, 36 (2005) 1707–1715.
- [27] Z.Y. Zhang, M.O.W. Richardson, “Low velocity impact induced damage evaluation and its effect on the residual flexural properties of pultruded GRP composites”, *Composite Structures*, 81 (2007) 195–201.
 - [28] R. Ambu, F. Aymerich, F. Ginesu, P. Priolo, “Assessment of NDT interferometric techniques for impact damage detection in composite laminates”, *Composites Science and Technology*, 66 (2006) 199–205.
 - [29] J.F. Laliberte', C. Poon, P.V. Straznicky, A. Fahr, “Post-impact fatigue damage growth in fiber–metal laminates”, *International Journal of Fatigue*, 24 (2002) 249–256,
 - [30] Z.Y. Zhang, M.O.W. Richardson, “Visualisation of barely visible impact damage in polymer matrix composites using an optical deformation and strain”, *Composites: Part A*, 36 (2005) 1073–1078.